

## Research Article

# The Faint Young Sun Paradox: A Simplified Thermodynamic Approach

F. Angulo-Brown,<sup>1</sup> Marco A. Rosales,<sup>1</sup> and M. A. Barranco-Jiménez<sup>2</sup>

<sup>1</sup>Departamento de Física, Escuela Superior de Física y Matemáticas, Instituto Politécnico Nacional, UP Zacatenco, 07738 Mexico, DF, Mexico

<sup>2</sup>Departamento de Formación Básica, Escuela Superior de Cómputo, Instituto Politécnico Nacional, Avenida Juan de Dios Batiz s/n. Esquina M. Othón de Mendizabal UP Adolfo López Mateos, 07738 Mexico, DF, Mexico

Correspondence should be addressed to M. A. Barranco-Jiménez, mbarrancoj@ipn.mx

Received 15 December 2011; Revised 16 March 2012; Accepted 15 May 2012

Academic Editor: J. P. Rozelot

Copyright © 2012 F. Angulo-Brown et al. This is an open access article distributed under the Creative Commons Attribution License, which permits unrestricted use, distribution, and reproduction in any medium, provided the original work is properly cited.

Classical models of the Sun suggest that the energy output in the early stage of its evolution was 30 percent less than today. In this context, radiative balance alone between The Sun and the Earth was not sufficient to explain the early presence of liquid water on Earth's surface. This difficulty is called the faint young Sun paradox. Many proposals have been published to solve this paradox. In the present work, we propose an oversimplified finite-time thermodynamic approach that describes the air convective cells in the Earth atmosphere. This model introduces two atmospheric modes of thermodynamic performance: a first mode consisting in the maximization of the power output of the convective cells (maximum power regime) and a second mode that consists in maximizing a functional representing a good trade-off between power output and entropy production (the ecological regime). Within the assumptions of this oversimplified model, we present different scenarios of albedo and greenhouse effects that seem realistic to preserve liquid water on the Earth in the early stage of formation.

## 1. Introduction

The so-called faint young Sun paradox [1] is a key drawback in the understanding of the early conditions of the Earth as well as the Sun's history itself [1, 2]. Such a paradox can be summarized as follows: the luminosity of the Sun, approximately 4.5–3.8 Gyr ago, was about 70–80 percent of its present value [1–7], which accounts only for terrestrial temperatures below the freezing point of water. As is well known, the Earth's surface temperature is mainly driven by the flux of solar radiation it receives and the interaction of radiation with atmosphere gases. In fact, assuming a black-body radiative balance between the young Sun and Earth results in  $T = 255\text{ K}$  [1], lower enough to have kept large parts of the Earth's surface frozen until 1-2 Gyr ago [4]. However, evidence from several independent lines of investigation suggests that for virtually its entire history Earth has maintained a surface temperature in the range within which water is a liquid, raising question about how

to reconcile these facts. Among the evidence for ancient liquid water temperatures at the Earth's surface is the dating of sedimentary rocks, that is, rocks laid down under water. These rocks date back to at least 4 Gyr before present (BP) [5–8]. On the other hand, Cogley and Henderson-Sellers [9], based on fossil studies, assert that liquid water would be necessary to explain the existence of diverse fossils in rocks dated earlier than 3.5 Gyr BP. More recently, Watson and Harrison [10], by studying ancient zircons from Western Australia, suggest that their results substantiate the existence of wet, minimum melting conditions at 4.55 to 4.0 Gyr BP. They further suggest that Earth had settled into a pattern of crust formation, erosion, and sediment recycling at that epoch.

Several approaches have been proposed to try to solve the faint young Sun paradox (FYSP) [1, 3–7, 11, 12]. Some solutions have usually involved higher amounts of greenhouse gases than the present in the modern-day atmosphere to compensate for the cooler Sun, for example, enhanced

amounts of CO<sub>2</sub> [13, 14], ammonia (NH<sub>3</sub>) [15], or methane (CH<sub>4</sub>) [16]. In 2003 [4], Shaviv proposed another FYSP solution by considering the cooling effect that cosmic rays are suspected to have on the global climate and that the younger Sun must have had a stronger solar wind (associated with a modest mass loss), such that it was more effective at stopping cosmic rays from reaching Earth. However, Bada et al. [11] have emphasized that FYSP proposals must include a scenario with a mechanism for melting a once frozen ocean. They proposed that bolide impacts between about 4.0 and 3.6 Gyr ago could have episodically melted an ice-covered early ocean.

Another kind of proposals have used alternative models of solar evolution (AMSE) originally constructed to explain the anomalous depletion of lithium in the Sun and similar stars [5, 6, 17]. These AMSE incorporate early solar mass loss of 5–10 percent predicting higher early solar luminosities [5] which have the potential to produce planetary temperatures within the liquid water range without requiring very high CO<sub>2</sub> concentrations [5]. Very recently, Turck-Chièze et al. [18], based on the study of rotational internal profile of the Sun, have shown that magnetic field has been probably present in the first stage with surface strong activity during the first million years and associated mass loss. These authors estimate the mass loss from the observations of young solar analogs which could reach up to 30 percent of the current mass. Although that phase is insufficiently described, it is not excluded that the initial luminosity would have been greater than standard solar model (SSM) results [18]. Regarding AMSE proposals, although Gaidos et al. [6] by observing  $\Pi^{01}$  Ursa Majoris, a 300-million-year-old solar-mass star (probable analog of the early Sun) placed an upper limit on the mass loss rate that possibly rules out AMSE as a solution of FYSP, the recent results by Turck-Chièze et al. [18] reinforce the feasibility of AMSE models.

Most of the previous FYSP proposed solutions have faced some form of contradictions or large uncertainties, either from geological data on atmospheric conditions or from atmospheric modeling [12]. For example, very high ancient CO<sub>2</sub> concentrations may prove to be inconsistent with derived weathering rates. Thus, as Graedel et al. [5] assert, the imposition of high CO<sub>2</sub> concentrations in Precambrian climate models is consistent with, but not required by, the temperature record. On the other hand, Hessler et al. [19] analyzed weathering rinds at river gravels dated back to 3.2 Gyr suggesting a lower limit of CO<sub>2</sub> partial pressure in the atmosphere to only several times the present value, which is two orders of magnitude below what is required to keep the surface temperature of Earth above freezing. In regard to high NH<sub>3</sub> concentrations [3, 15], Shaviv [4] asserts that, although not impossible, it is not easy to keep NH<sub>3</sub> from irreversibly photolyzing into H<sub>2</sub> and N<sub>2</sub> [20]. Shaviv also suggests that the CH<sub>4</sub> solution requires a long residency time of methane in the atmosphere and probable dominance of methanogenic bacteria, concluding that this type of solutions can neither be ruled out, nor proven at this point.

Recently von Paris et al. [12] reconsidered the role of CO<sub>2</sub> in warming the early Earth. They concluded that the amount of CO<sub>2</sub> needed to warm the surface of the early Earth

might have been overestimated by previous studies. They used a very detailed one-dimensional radiative-convective model based on several climate models to obtain CO<sub>2</sub> concentrations compatible with the amount inferred from sediment studies.

In summary, there exist a number of possible FYSP solutions stemming from distinct approaches, that is, distinct proposals that give liquid-water temperatures for the early Earth's surface.

In the present work, we also obtain liquid-water temperatures by means of an oversimplified finite-time thermodynamic model without the need of high concentrations of greenhouse gases. This approach is based on a highly idealized model that is not intended to provide a quantitatively accurate or physically complete description of the FYSP; that is, it is a toy model in the classification of Randall and Wielicki for models in atmospheric sciences [21]. It is necessary to emphasize that the convective cells of our model (as in the GZ-model [22]) are only virtual cells attempting to give a thermodynamically equivalent scheme of actual convection by means of taking into account the global thermodynamic restrictions over energy fluxes. However, we must mention that other oversimplified models can be found in books of climate dynamics [23]. These approaches can be 0D models based on changing the opacity and the number of effective layers of the atmosphere to compensate even very large changes of the solar constant in order to keep the surface temperature constant. See for example, the take-home exercise 11.2 from the classical text by Hartmann [23], where the FYSP is raised in terms of a greenhouse effect calculation, which leads to a very high normalized greenhouse coefficient (around 0.7). This result corresponds to a scenario that is not consistent with geological evidence [12, 24]. The present paper is organized as follows. In Section 2, we present a brief review of some basic concepts of finite-time thermodynamics (FTT); in Section 3, a simple model for wind energy as a solar-driven heat engine is discussed; in Section 4, an FTT-approach to the FYSP is proposed; finally in Section 5, we present some concluding remarks.

## 2. Finite-Time Thermodynamics

During the last decades, finite-time thermodynamics has extended its applications into many fields [26–32]. In the same way that early classical thermodynamics in the 19th century, starting from the study of thermal engines, soon reached practically all macroscopic systems, FTT went on to embrace many problems where entropy production of global processes plays an unavoidable role. For example, in a typical FTT heat engine model the whole entropy production is ascribed only to the coupling between the working substance and its surroundings, and it is permitted that the working fluid undergoes only reversible transformations. This approach is called the endoreversibility hypothesis (EH) [33]. By means of this hypothesis, it has been possible to place realistic bounds on irreversible processes that proceed in finite time. Usually, in FTT methodology one

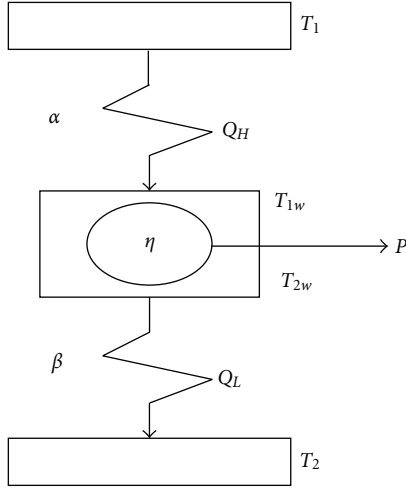
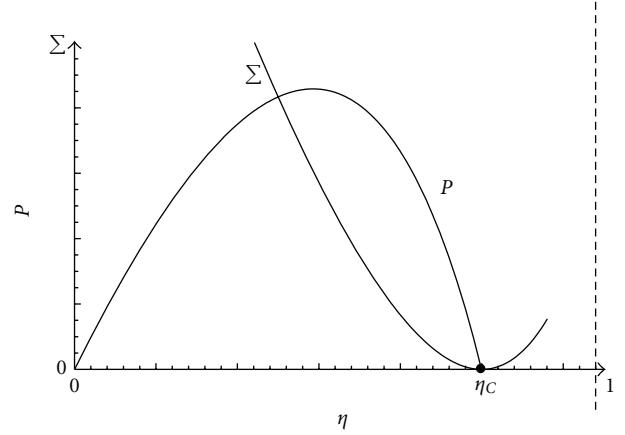


FIGURE 1: Curzon and Ahlborn heat engine.

calculates an extremum or optimum of a thermodynamically meaningful variable or functional [22]. Recently, Fischer and Hoffmann [34] showed that a simple endoreversible model (the so-called Novikov engine) can reproduce the complex engine behavior of a quantitative dynamical simulation of an Otto engine including, but not limited to, effects from losses due to heat conduction, exhaust losses, and frictional losses. On the other hand, Curto-Risso et al. [35] have published an FTT model also for an irreversible Otto cycle suitable to reproduce performance results of a very elaborated dynamical model of a real spark ignition heat engine including a turbulent flame propagation process, valves overlapping, heat transfer across the cylindrical walls, and a detailed analysis of the involved chemical reactions. In these two articles, the spirit of FTT is illustrated emphasizing the virtues and limitations of this methodology. However, in these articles, the usefulness of FTT models is shown beyond any doubt. In fact, we can assert that the FTT spirit is concomitant with the spirit of a Carnotian thermodynamics in the sense of the search for certain kind of limits for thermodynamic variables and functionals. For example, in 1975, Curzon and Ahlborn (hereafter CA) [36] published an article where they proposed a kind of Carnot cycle that produces entropy only due to an irreversible Newtonian heat transfer between two thermal reservoirs at absolute temperatures  $T_1$  and  $T_2$  ( $T_1 > T_2$ ) and the two isothermal branches of the working fluid at temperatures  $T_{1w}$  and  $T_{2w}$  ( $T_{1w} > T_{2w}$ ), respectively (see Figure 1) given by

$$\begin{aligned} Q_H &= \alpha(T_1 - T_{1w}), \\ Q_L &= \beta(T_{2w} - T_2), \end{aligned} \quad (1)$$

where  $\alpha$  and  $\beta$  are the thermal conductances of the materials that separate the reservoirs from the working substance and  $Q_H$  and  $Q_L$  are the heat flows per unit time. In this way, CA proposed an irreversible global model with  $\Delta S_{\text{tot}} > 0$  but internally reversible (EH). By integrating (1), CA obtained the cycle's period  $\Delta t$  and therefore they had a cycle with nonzero power, in contrast to the reversible

FIGURE 2:  $P$  versus  $\eta$  and  $\Sigma$  versus  $\eta$  for a CA cycle, (see [30, 38]).

Carnot cycle with both zero entropy and power productions. For the mentioned cycle model, CA maximized the power output and found that the efficiency under maximum-power conditions is expressed by

$$\eta_{\text{CA}} = 1 - \sqrt{\frac{T_2}{T_1}}. \quad (2)$$

The same expression was previously obtained by other authors [37]. Since the CA paper, many works have been published in the FTT-field [22, 26–42]. In Figure 2, it can be observed the qualitative behavior of both the power  $P$  and the entropy production  $\Sigma$  in terms of the efficiency  $\eta$ , for the Curzon-Ahlborn cycle [30]. From this figure it can be seen that the function

$$E = P - T_2 \Sigma \quad (3)$$

is a convex curve with a maximum point. This function was proposed by Angulo-Brown [38] and it has the following properties: at maximum  $E$ , the power output satisfies  $P_{E_{\text{max}}} \approx (3/4)P_{\text{max}}$ ; the entropy production is  $\Sigma_{E_{\text{max}}} \approx (1/4)\Sigma_{\text{max}}$ ; the efficiency is  $\eta_{E_{\text{max}}} \approx (1/2)(\eta_C + \eta_{\text{CA}})$ ,  $\eta_C$  being the Carnot efficiency. Due to the previous properties, the function given by (3) was named the ecological function, which pertains to the class of compromise functions between gains and losses mentioned by Greenspan [43]. The so-called ecological optimization has been applied in many areas. For instance, thermal engines [40], biochemical reactions [41, 42, 44, 45], linear energy converters [41, 42], superconducting transition [46], thermoeconomical optimization [47, 48], and atmospheric convective cells [49–51]. The ecological function given by (3) was later slightly modified by means of the inclusion of a parameter,  $\epsilon$ , which takes into account the particular heat transfer law employed in the thermal engine model [52, 53]. However, the mentioned “ecological” properties of the modified  $E$  do not appreciably change.

### 3. Wind Energy as a Solar-Driven Heat Engine

The problem of thermal balance between the planets of the solar system and the Sun under a FTT approach has

been treated by several authors [22, 30, 49, 51, 54, 55]. In some of these articles, the question of conversion of the solar energy into wind energy is also treated. As is well known [56], cosmic radiation, starlight, and moonlight can be neglected for the thermal balance of any of the planets of the solar system and only the following quantities have an influence: the incident solar influx or solar constant  $S$ , the dimensionless planet's albedo  $\rho$ , and the greenhouse effect of the planet's atmosphere crudely evaluated by means of a coefficient  $\gamma$ . This coefficient can be taken as the normalized greenhouse effect introduced by Raval and Ramanathan [57], which is defined as the infrared radiation energy trapped by the atmospheric gases and clouds. When only the global thermal balance between the Sun and a planet is considered, one can roughly obtain the planet's surface temperature assumed to be a uniform temperature  $T_p$ .

If the conversion of solar energy into wind energy is to be modeled, it is necessary to involve at least two representative atmospheric temperatures for making the creation of work possible, that is, to take the planet's atmosphere as a working fluid that converts heat into mechanical work. This permits to introduce in a natural way the concept of atmospheric "heat engine" (recently, Lucarini [58] has remarked the importance of this kind of two-temperature models for climate system analysis through an equivalent atmospheric Carnot engine). Within this context, process variables like work rate, heat fluxes, and efficiency, for instance, find a simple theoretical framework, where thermodynamical restrictions play a major role. This is in contrast with disciplines as nonequilibrium thermodynamics and hydrodynamics based on local differential equations where the transition from local to global variables is not a trivial task [54].

In 1989, Gordon and Zarmi (GZ) [22] introduced a FTT model taking the Sun-Earth-Wind system as a FTT cyclic heat engine where the heat input is the solar radiation, the working fluid is the Earth's atmosphere, and the energy in the winds is the work produced. The cold reservoir to which the engine rejects heat is the 3 K surrounding universe. By means of this oversimplified model, Gordon and Zarmi were able to obtain reasonable values for the annual average power in Earth's winds and for the average maximum and minimum temperatures of the atmosphere, without resorting to detailed dynamic models of the Earth's atmosphere, and without considering any other effect (such as Earth's rotation, Earth's translation around the Sun, and ocean currents). We wish to remark that the oversimplifications of this atmospheric model do not consider horizontal thermal gradients which affect the midlatitude and high-latitude air circulation or the unstable motions. The only heat transfer mechanism taken into account in the GZ model is the radiation. Other mechanisms such as latent heat transport are also not considered. Later, De Vos and Flater [56] extended the GZ-model to take into account the wind energy dissipation. In [59] the previous model was extended by including convective Hadley cells.

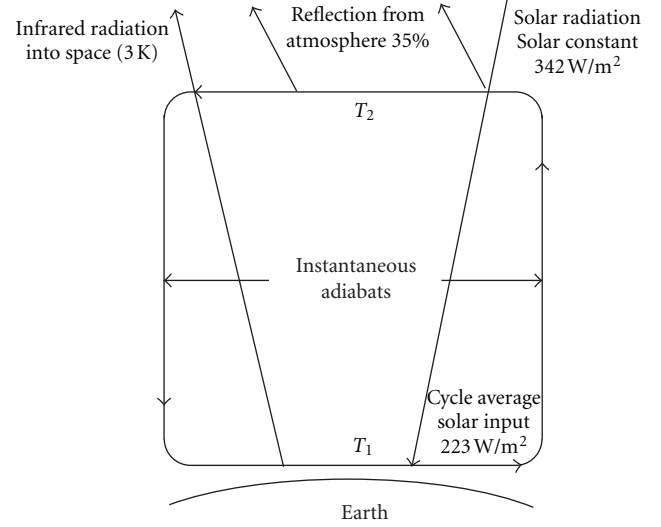


FIGURE 3: Schematic of a simplified solar-driven heat engine taken from [22].

**3.1. The Gordon-Zarmi Model.** In Figure 3, a schematic view of a simplified Sun-Earth-Wind system as a heat engine cycle is depicted (GZ-model). The cycle consists of four branches: two isothermal branches, one in which the atmosphere absorbs solar radiation at low altitudes and the other in which the atmosphere rejects heat at high altitudes to the universe, and two intermediate instantaneous adiabats with rising and falling air currents [22].

According to GZ, this oversimplified Carnot-like engine corresponds very approximately to the global scale motion of wind in convective cells. In what follows, we use all of GZ model assumptions. For instance, the work performed by the working fluid in one cycle  $W$ , the internal energy of the working fluid  $U$ , and the yearly average solar radiation flux  $q_s$  are expressed per unit area of Earth's surface. The temperatures of the four-branch cycle are taken as follows:  $T_1$  is the working fluid temperature in the isothermal branch at lowest altitude, where the working fluid absorbs solar radiation for half of the cycle, during the second half of the cycle heat is rejected via black-body radiation from the working fluid at temperature  $T_2$  (highest altitude of the cell) to the cold reservoir at temperature  $T_{ex}$  (the 3 K surrounding universe). In the GZ-model the objective is to maximize the work per cycle (average power) subject to the endoreversibility constraint [33], that is,

$$\Delta S_{\text{int}} = \int_0^{t_0} \left( \frac{q_s(t) - \sigma [T^4(t) - T_{\text{ex}}^4(t)]}{T(t)} \right) dt = 0, \quad (4)$$

where  $\Delta S_{\text{int}}$  is the change in entropy per unit area,  $t_0$  is the time of one cycle,  $\sigma$  is Stefan-Boltzmann constant

$(5.67 \times 10^{-8} \text{ W/m}^2\text{K}^4)$ , and  $q_s$ ,  $T$ , and  $T_{\text{ex}}$  are functions of time  $t$ , taken from [22]

$$T(t) = \begin{cases} T_1, & 0 \leq t \leq \frac{t_0}{2}, \\ T_2, & \frac{t_0}{2} \leq t \leq t_0, \end{cases} \quad (5)$$

$$T_{\text{ex}} = 3 \text{ K}, \quad 0 \leq t \leq t_0,$$

$$q_s(t) = \begin{cases} 0 & \frac{t_0}{2} \leq t \leq t_0, \\ \frac{S_0(1-\rho)}{2} & 0 \leq t \leq \frac{t_0}{2}, \end{cases}$$

with  $S_0$  the yearly average solar constant ( $1373 \text{ W/m}^2$ ) and  $\rho \approx 0.35$  [22] are the effective average albedo of the earth's atmosphere. The GZ model maximizes the work per cycle  $W$  (average power  $P$ ), taken from the first law of thermodynamics for one cycle

$$\Delta U = -W + \int_0^{t_0} (q_s(t) - \sigma[T^4(t) - T_{\text{ex}}^4(t)]) dt = 0 \quad (6)$$

by means of the Euler-Lagrange formalism and denoting average values as

$$\bar{T} = \frac{T_1 + T_2}{2},$$

$$\bar{T}^n = \frac{T_1^n + T_2^n}{2}, \quad (7)$$

$$\bar{q}_s = S_0 \frac{(1-\rho)}{4}.$$

From (6) and (7) and taking into account the constraint given by (4), GZ construct the following Lagrangian ( $L$ ):

$$L = T^4(t) + \lambda \left[ \frac{q_s(t)}{T(t)} - \sigma T^3(t) \right], \quad (8)$$

where  $\lambda$  is a Lagrange multiplier. By finding the extremum of  $L$  by means of  $\partial L / \partial T(t) = 0$ , GZ found for the Earth's atmosphere the following values:  $T_1 = 277 \text{ K}$ ,  $T_2 = 192 \text{ K}$  and  $P_{\text{max}} = W_{\text{max}}/t_0 = 17.1 \text{ W/m}^2$ . These numerical values are not so far from the "actual" values, which are  $P \approx 7 \text{ W/m}^2$  [60],  $T_1 \approx 290 \text{ K}$  (at ground level), and  $T_2 \approx 195 \text{ K}$  (at an altitude of around 75–90 km). However, as GZ assert, their power calculation must be taken as an upper bound due to several idealizations in their model. Later [49], the GZ-model was used to maximize the ecological function given by (3). This was made for both an endoreversible and a nonendoreversible cases. For the endoreversible case (with a 3 K surrounding universe) the following values were obtained:  $T_1 = 294 \text{ K}$ ,  $T_2 = 109.5 \text{ K}$ , and  $P_{\text{max}} = 6.89 \text{ W/m}^2$ , which are also good values, remarkably for  $T_1$  and  $P$ . Another endoreversible case was proposed in [49], but using as cold reservoir the tropopause layer with  $T_{\text{ex}} \approx 200 \text{ K}$ . In that case the numerical results were  $T_1 = 293.3 \text{ K}$ ,  $T_2 = 239.2 \text{ K}$ , and  $P_{\text{max}} = 10.75 \text{ W/m}^2$ , which are also reasonable values for the troposphere characteristics. The nonendoreversible version of the GZ model was accomplished by means of

a lumped nonendoreversibility parameter  $R$  which may be considered as a measure of the departure from an endoreversible regime, due to internal losses [61, 62]. This parameter arises from Clausius' inequality [63–65]. With this approach,  $T_1$ ,  $T_2$ , and  $P$  also reach reasonable values. When the nonendoreversibility parameter  $R$  and the greenhouse factor  $\gamma$  are considered, the integral constraint given by (4) must be modified, becoming

$$\Delta S_R = \int_0^{t_0} \left( \frac{q_s(t) - \sigma(1-\gamma)R[T^4(t) - T_{\text{ex}}^4(t)]}{T(t)} \right) dt = 0, \quad (9)$$

and the first law of thermodynamics applied over one cycle becomes

$$\Delta U = -W + \int_0^{t_0} (q_s(t) - \sigma(1-\gamma)[T^4(t) - T_{\text{ex}}^4(t)]) dt = 0. \quad (10)$$

By substituting (5) into (10), by considering that the factor  $(1-\gamma)$  corresponding to the greenhouse effect only participates in the lower half of the cycle depicted in Figure 3, and by integrating (10) with the approximation  $\bar{q}_s \gg \sigma T_{\text{ex}}^4$ , the expression for the average power output becomes

$$P = \bar{q}_s - \frac{\sigma}{2} [(1-\gamma)T_1^4 + T_2^4]. \quad (11)$$

With the same previous assumptions for the greenhouse effect, the integral constraint (9) turns out to be

$$\frac{\bar{q}_s}{T_1} = \frac{\sigma R}{2} [(1-\gamma)T_1^3 + T_2^3]. \quad (12)$$

Thus, for the maximization of the power output, we construct the following Lagrangian:

$$L'_R = \bar{q}_s - \frac{\sigma}{2} [(1-\gamma)T_1^4 + T_2^4] - \lambda \left\{ \frac{\bar{q}_s}{T_1} - \frac{\sigma R}{2} [(1-\gamma)T_1^3 + T_2^3] \right\}, \quad (13)$$

where  $\lambda$  is a Lagrange multiplier. From (13), by means of the Euler-Lagrange formalism, we obtain the following three equations:

$$T_1^5 - \frac{3}{4} R \lambda T_1^4 - \frac{\bar{q}_s}{2\sigma(1-\gamma)} \lambda = 0,$$

$$\lambda = \frac{4}{3R} T_2, \quad (14)$$

$$T_1^4 - \frac{1}{(1-\gamma)} T_1 T_2^3 - \frac{2\bar{q}_s}{\sigma R(1-\gamma)} = 0,$$

which, by the elimination of  $\lambda$ , reduce to

$$T_1^5 - T_2 T_1^4 - \frac{2\bar{q}_s}{3\sigma R(1-\gamma)} T_2 = 0,$$

$$T_1^4 - \frac{1}{(1-\gamma)} T_1 T_2^3 - \frac{2\bar{q}_s}{\sigma R(1-\gamma)} = 0. \quad (15)$$

The numerical solutions of (15) give us the low altitude temperature  $T_1$  and the high altitude temperature  $T_2$  for an atmospheric "heat engine" operating under maximum power conditions.

3.2. *The Maximum-Ecological Regime.* If the objective is the maximization of the so-called ecological function given by (3), first, we need to calculate the mean entropy production per cycle of the thermodynamic universe,  $\Delta S_u/t_0$ . Starting from Figure 3, we have

$$\Delta S_u = \int_0^{t_0} \left( \frac{-q_s(t) + \sigma(1-\gamma)R[T^4(t) - T_{\text{ex}}^4(t)]}{T(t)} \right) dt. \quad (16)$$

If we consider the greenhouse effect only in the first half of the cycle, by means of (5), we get

$$\begin{aligned} \Delta S_u = & \int_0^{t_0/2} \left( \frac{(S_0(1-\rho)/2) + \sigma(1-\gamma)R[T_1^4 - T_{\text{ex}}^4]}{T_1} \right) dt \\ & + \int_{t_0/2}^{t_0} \left( \frac{\sigma R[T_2^4 - T_{\text{ex}}^4]}{T_{\text{ex}}} \right) dt, \end{aligned} \quad (17)$$

$$\frac{\Delta S_u}{t_0} = -\frac{\bar{q}_s}{T_1} + \frac{\sigma R}{2} \left[ (1-\gamma)T_1^3 + \frac{T_2^4}{T_{\text{ex}}} \right], \quad (18)$$

where we have used the approximation,  $\bar{q}_s \gg \sigma T_{\text{ex}}^4$ . Therefore, by the substitution of (11) and (18) into (3), the ecological function  $E$  becomes

$$\begin{aligned} E = & \bar{q}_s - \frac{\sigma}{2} [(1-\gamma)T_1^4 + T_2^4] + \frac{T_{\text{ex}}\bar{q}_s}{T_1} \\ & - \frac{\sigma R T_{\text{ex}}}{2} \left[ (1-\gamma)T_1^3 + \frac{T_2^4}{T_{\text{ex}}} \right]. \end{aligned} \quad (19)$$

Then, we propose the following Lagrangian,

$$\begin{aligned} L_E = & \bar{q}_s - \frac{\sigma}{2} [(1-\gamma)T_1^4 + T_2^4] + \frac{T_{\text{ex}}\bar{q}_s}{T_1} \\ & - \frac{\sigma R T_{\text{ex}}}{2} \left[ (1-\gamma)T_1^3 + \frac{T_2^4}{T_{\text{ex}}} \right] \\ & - \lambda \left\{ \frac{\bar{q}_s}{T_1} - \frac{\sigma R}{2} [(1-\gamma)T_1^3 + T_2^3] \right\}, \end{aligned} \quad (20)$$

where  $\lambda$  is a Lagrange multiplier and the constraint given by (12) has been used. By solving the Euler-Lagrange equations for this Lagrangian, we obtain

$$\begin{aligned} T_1^5 + \left[ \frac{3T_{\text{ex}}}{4}R - (1+R)T_2 \right] T_1^4 - \frac{2\bar{q}_s}{3\sigma} \left( \frac{1+R}{R} \right) \left( \frac{1}{1-\gamma} \right) T_2 \\ + \frac{T_{\text{ex}}\bar{q}_s}{2\sigma} \left( \frac{1}{1-\gamma} \right) = 0, \\ T_1^4 + \frac{1}{(1-\gamma)} T_1 T_2^3 - \frac{2\bar{q}_s}{\sigma R} \left( \frac{1}{1-\gamma} \right) = 0. \end{aligned} \quad (21)$$

To summarize, by solving (15) for the maximum power regime (MPR) and (21) for the maximum ecological regime (MER), we can obtain the surface temperature  $T_1$  and the high altitude temperature  $T_2$  for both scenarios (MPR and

MER). The altitude corresponding to  $T_2$  strongly depends on which layer we use as cold reservoir. For the cases of atmospheres with a tropopause layer,  $T_2$  reaches very realistic values within tropospheric characteristics [51].

#### 4. A FTT-Approach to the Faint Young Sun Paradox

We take as the first hypothesis that solar radiation has increased over the main-sequence lifetime of the Sun due to the increase in the mean density of the solar core as hydrogen is converted into helium. In all the standard solar models (SSM) [25], the luminosity of the young Sun was estimated 30% less than the present value. According to Gough [3], the rate of increase of luminosity with time,  $t$ , can be expressed as

$$S(t) = \left[ 1 + 0.4 \left( 1 - \frac{t}{t_0} \right) \right]^{-1} S_0, \quad (22)$$

where  $S_0$  is the present solar luminosity and  $t_0$  ( $\approx 4.56$  Gyrs) is the present age of the Sun. Equations (15) and (21) necessary to calculate  $T_1$  and  $T_2$  under both MPR and MER scenarios use the following as input data: the cold reservoir temperature  $T_{\text{ex}}$  (the 3 K surrounding universe, which could be up to 9.5 K 12 Gyr ago [66]) the solar luminosity  $S(t)$  and the effective average albedo  $\rho$  both combined through the yearly average solar radiation flux  $q_s = S_0(1-\rho)/2$ ; the greenhouse coefficient  $\gamma$ ; the nonendoreversibility parameter  $R$ . In principle,  $S(t)$  is taken as governed by Gough equation (22).

In Table 1, we show the numerical results for an atmosphere working under the MP-regime for several parameter values. The present-day values for average albedo and the greenhouse parameter are  $\rho \approx 0.3$  and  $\gamma = 0.4$ , respectively. For the Earth,  $\gamma$  is a normalized greenhouse effect parameter defined as  $\gamma = (E_s - F)/E_s$  [57], where  $E_s$  is the surface emission and  $F$  is the outgoing radiation. As we can see for a low  $\rho$  and a low  $\gamma$  scenario (first row), we can obtain liquid-water temperatures around 4.5–3.6 Gyr ago for solar constants within the interval  $[0.7S_0, 0.8S_0]$ . In this case  $\rho = 0.17$  is a half of the present value and  $\gamma = 0.06$  a seventh of the present value, that is, a scenario with small concentration values of greenhouse gases. In Table 1, we also observe several other possible scenarios for combinations of  $\rho$  and  $\gamma$  values. For the first row in Table 1 we use a value of  $R = 0.95$ , that is, an internally nonendoreversible convective cell model, taking into account in a lumped manner some internal dissipations [61, 62]. The sixth column corresponds to surface temperatures estimated for  $S(t)$  values taken from Table 11 of [25]. As can be seen in sixth column, also for this model we find liquid-water temperatures in early stages of Earth's surface. In fact, these surface temperatures are larger than those obtained with Gough's curve (see Figure 4, for a comparison of both curves). In Table 2, we present several possible scenarios of an Earth's atmosphere working under the ME regime. Here, we also obtain that for relatively small values of  $\rho$  and  $\gamma$  it is possible to find liquid-water temperatures for the young Earth, by considering the

TABLE 1: Possible scenarios of ancient surface temperatures under maximum power output regime. Input data:  $\rho$ ,  $\gamma$ ,  $R$  (one case).  $S/S_0$  is calculated according to Gough equation for a given age. The fifth column corresponds to our calculated temperatures. For the first row data  $R = 0.95$  was considered. The sixth column shows the surface temperatures estimated from  $S(t)$  values reported in Table 11 of [25].

Albedo $\rho$	Greenhouse coefficient $\gamma$	Solar constant $S/S_0$ (normalized)	Time BP (Gyr)	Surface temperature, $T_1$ (K)	Surface temperature, $T_1$ (K)
0.17	0.06	0.7-0.8	4.5-3.6	273.7-283.04	280.1-283.01
0.25	0.15	0.72	4.47	273.7	280.33
0.30	0.20	0.74	4.04	273.1	279.74
0.35	0.30	0.72	4.47	273.8	280.01
0.40	0.35	0.73	4.25	273.1	280.03

TABLE 2: Possible scenarios of ancient surface temperatures under maximum ecological conditions. For the first row data  $R = 0.95$  was considered.

Albedo $\rho$	Greenhouse coefficient $\gamma$	Solar constant $S/S_0$ (normalized)	Time BP (Gyr)	Surface temperature, $T_1$ (K)
0.17	0.06	0.7-0.8	4.5-3.6	293.6-303.6
0.40	0.0	0.81	2.297	273.1
	0.1	0.73	4.253	273.0
0.45	0.0	0.88	1.568	273.1
	0.1	0.80	2.875	273.2
	0.15	0.76	3.631	273.4
	0.20	0.71	4.697	273.7
0.50	0.1	0.88	1.568	273.2
	0.15	0.83	2.355	273.3
	0.20	0.79	3.056	373.5
	0.25	0.74	4.045	273.1

way of thermodynamic performance of the atmosphere in addition to the  $\rho$  and  $\gamma$  values. The FTT-approach here presented is mainly based on the role played by the global behavior of the Earth's atmosphere and its mode of using the input of solar energy in order to propose the values of both albedo and greenhouse parameters which produce surface temperatures,  $T_1$ , above the freezing point of water. In Table 3 (for MP regime) and Table 4 (for ME regime) we show a similar calculation for Mars' atmosphere by using several combinations of  $\rho$  and  $\gamma$  parameters. In this case, we also find liquid-water temperatures corresponding to early stages of the Sun, mainly for the ecological way of thermodynamic performance.

## 5. Concluding Remarks

In Tables 1 and 2 for Earth and Tables 3 and 4 for Mars, we present several possible scenarios for values of both albedo and greenhouse parameters ( $\rho$  and  $\gamma$ ), which produce surface temperatures above the freezing point of water. For the case of the Earth, the temperatures for some ages are compatible with recent geological evidence of possible ancient existence of liquid water on Earth. Remarkably, in our approach only moderate and low values of greenhouse effect and albedo are necessary to produce early liquid-water temperatures. Our model is mainly based on the role played by the global thermodynamical behavior of the atmosphere and on its mode of using the input of solar energy. As asserted by Pierrehumbert [67], the planetary warming resulting from

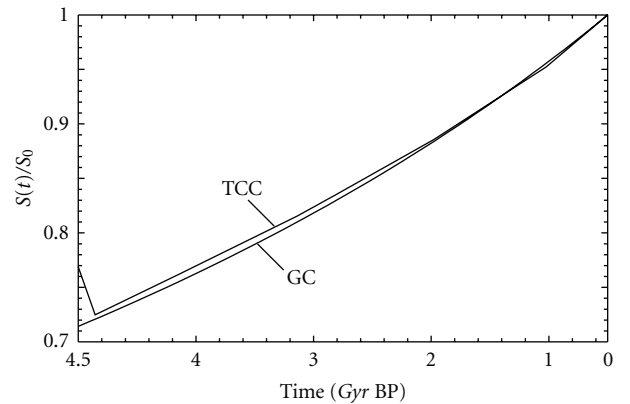


FIGURE 4: Comparison between Gough curve ((22), GC) and Turck-Chièze et al. curve (TCC) depicted with  $S(t)/S_0$  values taken from Table 11 of [25]. Both curves correspond to solar models without mass loss in the early stage of the Sun.

the greenhouse (and albedo) effect is consistent with the second law of thermodynamics because a planet is not a closed system. It exchanges heat with a high-temperature bath by absorbing radiation from the photosphere of its star and with a cold bath by emitting IR into the essentially zero-temperature reservoir of space. The so-called ‘‘ecological’’ scenarios offer a better range of greenhouse and albedo combinations than the ‘‘maximum power’’ scenarios with respect to a possible solution of the faint young Sun paradox.

TABLE 3: Possible scenarios of ancient surface temperatures for Mars under maximum power output regime.

Albedo $\rho$	Greenhouse coefficient $\gamma$	Solar constant $S/S_0$ (normalized)	Time BP (Gyr)	Surface temperature, $T_1$ (K)
0.0	0.5	0.85	2.029	275.2
0.1	0.5	0.95	0.66	272.9

TABLE 4: Possible scenarios of ancient surface temperatures for Mars under maximum ecological function conditions.

Albedo $\rho$	Greenhouse coefficient $\gamma$	Solar constant $S/S_0$ (normalized)	Time BP (Gyr)	Surface temperature, $T_1$ (K)
0.0	0.2	0.9	1.277	273.4
0.0	0.3	0.8	2.875	273.9
0.1	0.3	0.9	1.310	274.0
0.1	0.4	0.9	3.631	273.1
0.2	0.3	0.99	0.116	273.2
0.2	0.4	0.86	1.872	273.4
0.2	0.5	0.73	4.25	273.7
0.3	0.4	0.98	0.234	273.2
0.3	0.5	0.83	2.355	273.3
0.4	0.6	0.8	2.875	274.1

Although our model only uses average lumped parameters and general thermodynamic restrictions, it leads to results qualitatively compatible with those recently published by von Paris et al [12], which were obtained by means of a very detailed climate model. Very recently, Goldblatt et al. [68] have published an outstanding proposal on the FYSP. They suggest that a higher nitrogen level in the early atmosphere probably helped warm the early Earth by means of an increase in the atmosphere pressure stemming from  $N_2$ , which would have augmented the warming effect of existing greenhouse gases, by broadening their absorption lines. In 2010, Rosing et al. [24] have proposed that the mineralogy of Archean (3.8 to 2.5 Gyr ago) sediments is inconsistent with high concentrations of greenhouse gases and the metabolic constraints of extant methanogens. Prompted by this, they hypothesize that a lower albedo on the Earth made an important contribution to moderating surface temperature in the Archean eon. In fact, they used albedos around 0.10 to 0.26, which are numbers consistent with those used in our calculations. In summary, our oversimplified model using the hypotheses of a faint young Sun does not face important contradictions with other solutions recently proposed. Of course we shall find even easier solutions for AMSE models based on mass loss observed in young stars and suggested by helioseismological data [18, 25, 69].

## Acknowledgments

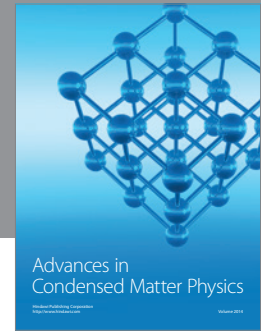
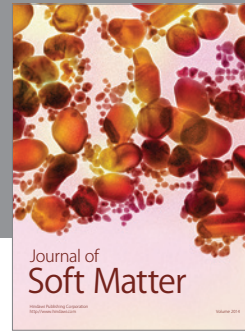
The authors gratefully acknowledge R. Hernández-Pérez and T. E. Govindan for revising the paper. F. A. Brown and M. A. Barranco-Jiménez thank the financial support by CONACYT, COFAA and EDI-IPN-México. This paper is dedicated to the memory of Marco A. Rosales.

## References

- [1] C. Sagan and G. Mullen, “Earth and Mars: evolution of atmospheres and surface temperatures,” *Science*, vol. 177, no. 4043, pp. 52–56, 1972.
- [2] J. F. Kasting and D. H. Grinspoon, “The faint young Sun problem,” in *The Sun in Time*, pp. 447–462, The University of Arizona, Tucson, Ariz, USA, 1991.
- [3] D. O. Gough, “Solar interior structure and luminosity variations,” *Solar Physics*, vol. 74, no. 1, pp. 21–34, 1981.
- [4] N. J. Shaviv, “Toward a solution to the early faint Sun paradox: a lower cosmic ray flux from a stronger solar wind,” *Journal of Geophysical Research A*, vol. 108, no. 12, article 1437, 8 pages, 2003.
- [5] T. Graedel, I. J. Sackmann, and A. Boothroyd, “Early solar mass loss: a potential solution to the weak sun paradox,” *Geophysical Research Letters*, vol. 18, pp. 1881–1884, 1991.
- [6] E. J. Gaidos, M. Güdel, and G. A. Blake, “The faint young sun paradox: an observational test of an alternative solar model,” *Geophysical Research Letters*, vol. 27, no. 4, pp. 501–503, 2000.
- [7] D. A. Minton and R. Malhotra, “Assessing the massive young SUN hypothesis to solve the warm young earth puzzle,” *Astrophysical Journal*, vol. 660, no. 2, pp. 1700–1706, 2007.
- [8] S. A. Bowring, I. S. Williams, and W. Compston, “3.96 Ga gneisses from the Slave province, Northwest Territories, Canada,” *Geology*, vol. 17, no. 11, pp. 971–975, 1989.
- [9] J. G. Cogley and A. Henderson-Sellers, “The origin and earliest state of the earth’s hydrosphere,” *Reviews of Geophysics & Space Physics*, vol. 22, no. 2, pp. 131–175, 1984.
- [10] E. B. Watson and T. M. Harrison, “Zircon thermometer reveals minimum melting conditions on earliest earth,” *Science*, vol. 308, no. 5723, pp. 841–844, 2005.
- [11] J. L. Bada, C. Bigham, and S. L. Miller, “Impact melting of frozen oceans on the early Earth: implications for the origin of life,” *Proceedings of the National Academy of Sciences of the United States of America*, vol. 91, no. 4, pp. 1248–1250, 1994.

- [12] P. von Paris, H. Rauer, J. Lee Grenfell et al., "Warming the early earth-CO<sub>2</sub> reconsidered," *Planetary and Space Science*, vol. 56, no. 9, pp. 1244–1259, 2008.
- [13] W. R. Kuhn and J. F. Kasting, "Effects of increased CO<sub>2</sub> concentrations on surface temperature of the early Earth," *Nature*, vol. 301, no. 5895, pp. 53–55, 1983.
- [14] J. F. Kasting, "Earth's early atmosphere," *Science*, vol. 259, pp. 920–926, 1993.
- [15] C. Sagan and C. Chyba, "The early faint sun paradox: organic shielding of ultraviolet-labile greenhouse gases," *Science*, vol. 276, no. 5316, pp. 1217–1221, 1997.
- [16] A. A. Pavlov, J. F. Kasting, L. L. Brown, K. A. Rages, and R. Freedman, "Greenhouse warming by CH<sub>4</sub> in the atmosphere of early Earth," *Journal of Geophysical Research E*, vol. 105, no. 5, pp. 11981–11990, 2000.
- [17] H. D. Holland, B. Lazar, and M. McCaffrey, "Evolution of the atmosphere and oceans," *Nature*, vol. 320, no. 6057, pp. 27–33, 1986.
- [18] S. Turck-Chièze, L. Piau, and S. Couvidat, "The solar energetic balance revisited by young solar analogs, helioseismology, and neutrinos," *The Astrophysical Journal Letters*, vol. 731, no. 2, article L29, 2011.
- [19] A. M. Hessler, D. R. Lowe, R. L. Jones, and D. K. Bird, "A lower limit for atmospheric carbon dioxide levels 3.2 billion years ago," *Nature*, vol. 428, no. 6984, pp. 736–738, 2004.
- [20] J. F. Kasting, "Stability of ammonia in the primitive terrestrial atmosphere," *Geophysical Research Letters*, vol. 87, pp. 3091–3058, 1982.
- [21] D. A. Randall and B. A. Wielicki, "Measurements, models, and hypotheses in the atmospheric sciences," *Bulletin of the American Meteorological Society*, vol. 78, no. 3, pp. 399–406, 1997.
- [22] M. Gordon and Y. Zarmi, "Wind energy as a solar-driven heat engine: a thermodynamic approach," *American Journal of Physics*, vol. 57, pp. 995–998, 1989.
- [23] D. L. Hartmann, *Global Physical Climatology*, Academic Press, London, UK, 1994.
- [24] M. T. Rosing, D. K. Bird, N. H. Sleep, and C. J. Bjerrum, "No climate paradox under the faint early Sun," *Nature*, vol. 464, no. 7289, pp. 744–747, 2010.
- [25] S. Turck-Chièze, W. Däppen, E. Fossat, J. Provost, E. Schatzman, and D. Vignaud, "The solar interior," *Physics Report*, vol. 230, no. 2–4, pp. 57–235, 1993.
- [26] A. Bejan, "Entropy generation minimization: the new thermodynamics of finite-size devices and finite-time processes," *Journal of Applied Physics*, vol. 79, no. 3, pp. 1191–1218, 1996.
- [27] W. Chih, L. Chen, and J. Chen, *Recent Advances in Finite Time Thermodynamics*, Nova Science, New York, NY, USA, 1999.
- [28] A. Durmayaz, O. S. Sogut, B. Sahin, and H. Yavuz, "Optimization of thermal systems based on finite-time thermodynamics and thermoeconomics," *Progress in Energy and Combustion Science*, vol. 30, no. 2, pp. 175–217, 2004.
- [29] S. Sieniutycz and P. Salamon, *Advances in Thermodynamics*, vol. 4 of *Finite-Time Thermodynamics and Thermoeconomics*, CRC & Taylor & Francis, New York, NY, USA, 1990.
- [30] A. DeVos, *Endoreversible Thermodynamics of Solar Energy Conversion*, Oxford University Press, New York, NY, USA, 1992.
- [31] L. Chen and F. Sun, *Advances in Finite Time Thermodynamics*, Nova Science, New York, NY, USA, 2004.
- [32] K. H. Hoffmann, J. M. Burzler, and S. Schubert, "Endoreversible thermodynamics," *Journal of Non-Equilibrium Thermodynamics*, vol. 22, no. 4, pp. 311–355, 1997.
- [33] M. H. Rubin, "Optimal configuration of a class of irreversible heat engines. I," *Physical Review A*, vol. 19, no. 3, pp. 1272–1276, 1979.
- [34] A. Fischer and K. H. Hoffmann, "Can a quantitative simulation of an Otto engine be accurately rendered by a simple Novikov model with heat leak?" *Journal of Non-Equilibrium Thermodynamics*, vol. 29, no. 1, pp. 9–28, 2004.
- [35] P. L. Curto-Risso, A. Medina, and A. C. Hernández, "Theoretical and simulated models for an irreversible Otto cycle," *Journal of Applied Physics*, vol. 104, no. 9, Article ID 094911, 2008.
- [36] F. Curzon and B. Ahlborn, "Efficiency of a carnot engine at maximum power output," *American Journal of Physics*, vol. 43, pp. 22–24, 1975.
- [37] M. Feidt, M. Costea, C. Petre, and S. Petrescu, "Optimization of the direct Carnot cycle," *Applied Thermal Engineering*, vol. 27, no. 5–6, pp. 829–839, 2007.
- [38] F. Angulo-Brown, "An ecological optimization criterion for finite-time heat engines," *Journal of Applied Physics*, vol. 69, no. 11, pp. 7465–7469, 1991.
- [39] L. A. Arias-Hernández, *Algunas propiedades y aplicaciones del criterio de optimización ecológico en termodinámica fuera de equilibrio [Tesis Doctoral]*, Escuela Superior de Física y Matemáticas del IPN, País, Mexico, 2000.
- [40] L. Chen, W. Zhang, and F. Sun, "Power, efficiency, entropy-generation rate and ecological optimization for a class of generalized irreversible universal heat-engine cycles," *Applied Energy*, vol. 84, no. 5, pp. 512–525, 2007.
- [41] F. Angulo-Brown, M. Santillán, and E. Calleja-Quevedo, "Thermodynamic optimality in some biochemical reactions," *Il Nuovo Cimento D*, vol. 17, no. 1, pp. 87–90, 1995.
- [42] M. Santillán, L. A. Arias-Hernández, and F. Angulo-Brown, "Some optimization criteria for biological systems in linear irreversible thermodynamics," *Nuovo Cimento della Societa Italiana di Fisica D*, vol. 19, no. 1, pp. 99–109, 1997.
- [43] N. S. Greenspan, "You can't have it all," *Nature*, vol. 409, article 137, 2001.
- [44] L. A. Arias-Hernandez, F. Angulo-Brown, and R. T. Paez-Hernandez, "First-order irreversible thermodynamic approach to a simple energy converter," *Physical Review E*, vol. 77, no. 1, Article ID 011123, 8 pages, 2008.
- [45] O. Diaz-Hernández, R. Páez-Hernández, and M. Santillán, "Thermodynamic performance vs. dynamic stability in an enzymatic reaction model," *Physica A*, vol. 389, no. 17, pp. 3476–3483, 2010.
- [46] L. A. Arias-Hernandez, F. Angulo-Brown, and R. T. Paez-Hernandez, "First-order irreversible thermodynamic approach to a simple energy converter," *Physical Review E*, vol. 77, no. 1, Article ID 011123, 8 pages, 2008.
- [47] M. A. Barranco-Jiménez and F. Angulo-Brown, "Thermoeconomic optimisation of Novikov power plant model under maximum ecological conditions," *Journal of the Energy Institute*, vol. 80, no. 2, pp. 96–104, 2007.
- [48] M. A. Barranco-Jiménez and F. Angulo-Brown, "Thermoeconomic optimisation of endoreversible heat engine under maximum modified ecological criterion," *Journal of the Energy Institute*, vol. 80, no. 4, pp. 232–238, 2007.
- [49] M. A. Barranco-Jiménez and F. Angulo-Brown, "A nonendoreversible model for wind energy as a solar-driven heat engine," *Journal of Applied Physics*, vol. 80, no. 9, pp. 4872–4876, 1996.
- [50] M. A. Barranco-Jiménez, J. C. Chimal-Eguía, and F. Angulo-Brown, "The Gordon and Zarmi model for convective atmospheric cells under the ecological criterion applied to the

- planets of the solar system,” *Revista Mexicana de Fisica*, vol. 52, no. 3, pp. 205–212, 2006.
- [51] M. A. Barranco-Jiménez and F. Angulo-Brown, “A simple model on the influence of the greenhouse effect on the efficiency of solar-to-wind energy conversion,” *Nuovo Cimento della Societa Italiana di Fisica C*, vol. 26, no. 5, pp. 535–552, 2003.
- [52] F. Angulo-Brown and L. A. Arias-Hernández, “Reply to ‘comment on ‘a general property of endoreversible thermal engines’ [J. Appl. Phys. 89, 1518 (2001)],” *Journal of Applied Physics*, vol. 89, no. 2, pp. 1520–1521, 2001.
- [53] L. A. Arias-Hernández, G. Ares De Parga, and F. Angulo-Brown, “A variational ecological-type optimization of some thermal-engine models,” *Open Systems and Information Dynamics*, vol. 11, no. 2, pp. 123–138, 2004.
- [54] G. Pollarolo and L. Sertorio, “Energy and entropy balance for a black piecewise homogeneous planet,” *Il Nuovo Cimento C*, vol. 2, no. 3, pp. 335–351, 1979.
- [55] A. De Vos and P. van der Wel, “The efficiency of the conversion of solar energy into wind energy by means of Hadley cells,” *Theoretical and Applied Climatology*, vol. 46, no. 4, pp. 193–202, 1993.
- [56] A. DeVos and G. Flatter, “The maximum efficiency of the conversion of solar-energy into wind energy,” *American Journal of Physics*, vol. 59, pp. 751–754, 1991.
- [57] A. Raval and V. Ramanathan, “Observational determination of the greenhouse effect,” *Nature*, vol. 342, no. 6251, pp. 758–761, 1989.
- [58] V. Lucarini, “Thermodynamic efficiency and entropy production in the climate system,” *Physical Review E*, vol. 80, no. 2, Article ID 021118, 5 pages, 2009.
- [59] A. DeVos and P. van der Well, “Endoreversible models for the conversion of solar energy into wind energy,” *Journal of Non-Equilibrium Thermodynamics*, vol. 17, pp. 79–89, 1992.
- [60] M. R. Gustavson, “Limits to wind power utilization,” *Science*, vol. 204, no. 4388, pp. 13–17, 1979.
- [61] S. Ozkaynak, S. Goktun, and H. Yavuz, “Finite-time thermodynamic analysis of a radiative heat engine with internal irreversibility,” *Journal of Physics D*, vol. 27, no. 6, pp. 1139–1143, 1994.
- [62] J. Chen, “Maximum power output and maximum efficiency of an irreversible Carnot heat engine,” *Journal of Physics D*, vol. 27, no. 6, pp. 1144–1149, 1994.
- [63] S. Velasco, J. M. M. Roco, A. Medina, J. A. White, and A. Calvo Hernández, “Optimization of heat engines including the saving of natural resources and the reduction of thermal pollution,” *Journal of Physics D*, vol. 33, no. 4, pp. 355–359, 2000.
- [64] L. Chen, C. Wu, and F. Sun, “Finite time thermodynamic optimization or entropy generation minimization of energy systems,” *Journal of Non-Equilibrium Thermodynamics*, vol. 24, no. 4, pp. 327–359, 1999.
- [65] G. Ares De Parga, F. Angulo-Brown, and T. D. Navarrete-González, “A variational optimization of a finite-time thermal cycle with a nonlinear heat transfer law,” *Energy*, vol. 24, no. 12, pp. 997–1008, 1999.
- [66] R. Srianand, P. Petitjean, and C. Ledoux, “The microwave background temperature at the redshift of 2.33771,” *Natur*, vol. 408, pp. 931–934, 2000.
- [67] R. T. Pierrehumbert, “Infrared radiation and planetary temperature,” *Physics Today*, vol. 64, no. 1, pp. 33–38, 2011.
- [68] C. Goldblatt, M. W. Claire, T. M. Lenton, A. J. Matthews, A. J. Watson, and K. J. Zahnle, “Nitrogen-enhanced greenhouse warming on early earth,” *Nature Geoscience*, vol. 2, no. 12, pp. 891–896, 2009.
- [69] S. Turck-Chieze, S. Cahen, M. Cassé, and C. Doom, “Revisiting the standar solar model,” *The Astrophysical Journal Letters*, vol. 335, pp. 415–424, 1988.



**Hindawi**

Submit your manuscripts at  
<http://www.hindawi.com>

